

Flexible germanium nanomembrane metal-semiconductor-metal photodiodes

Munho Kim, Jung-Hun Seo, Zongfu Yu, Weidong Zhou, and Zhenqiang Ma

Citation: [Applied Physics Letters](#) **109**, 051105 (2016); doi: 10.1063/1.4960460

View online: <http://dx.doi.org/10.1063/1.4960460>

View Table of Contents: <http://scitation.aip.org/content/aip/journal/apl/109/5?ver=pdfcov>

Published by the [AIP Publishing](#)

Articles you may be interested in

[Flexible nanomembrane photonic-crystal cavities for tensilely strained-germanium light emission](#)

Appl. Phys. Lett. **108**, 241107 (2016); 10.1063/1.4954188

[Capacitance-voltage characteristics of Si and Ge nanomembrane based flexible metal-oxide-semiconductor devices under bending conditions](#)

Appl. Phys. Lett. **108**, 233505 (2016); 10.1063/1.4953458

[1.9% bi-axial tensile strain in thick germanium suspended membranes fabricated in optical germanium-on-insulator substrates for laser applications](#)

Appl. Phys. Lett. **107**, 191904 (2015); 10.1063/1.4935590

[Electroluminescence from strained germanium membranes and implications for an efficient Si-compatible laser](#)

Appl. Phys. Lett. **100**, 131112 (2012); 10.1063/1.3699224

[Evaluation of Schottky contact parameters in metal-semiconductor-metal photodiode structures](#)

Appl. Phys. Lett. **77**, 274 (2000); 10.1063/1.126948

A promotional banner for Applied Physics Reviews. On the left is a small image of the journal cover for 'Applied Physics Reviews', which features a diagram of a device structure. The main part of the banner has a blue background with a bright light source on the right. The text 'NEW Special Topic Sections' is prominently displayed in white. Below this, in an orange bar, it says 'NOW ONLINE' in yellow, followed by 'Lithium Niobate Properties and Applications: Reviews of Emerging Trends' in white. The AIP Applied Physics Reviews logo is in the bottom right corner.

NEW Special Topic Sections

NOW ONLINE
Lithium Niobate Properties and Applications:
Reviews of Emerging Trends

AIP Applied Physics Reviews

Flexible germanium nanomembrane metal-semiconductor-metal photodiodes

Munho Kim,^{1,a)} Jung-Hun Seo,¹ Zongfu Yu,¹ Weidong Zhou,² and Zhenqiang Ma^{1,b)}

¹Department of Electrical and Computer Engineering, University of Wisconsin at Madison, Madison, Wisconsin 53706, USA

²Department of Electrical Engineering, University of Texas at Arlington, Arlington, Texas 76019, USA

(Received 18 May 2016; accepted 23 July 2016; published online 2 August 2016)

We demonstrate flexible Ge nanomembrane (Ge NM) based metal-semiconductor-metal photodiodes. The effect of uniaxial tensile strain on Ge NM based photodiodes was investigated using bending fixtures. Dark current density is decreased from 21.5 to 4.8 mA/cm² at 3 V by a tensile strain of 0.42% while photon responsivity is increased from 0.2 to 0.45 A/W at the wavelength of 1.5 μ m. Enhanced responsivity is also observed at longer wavelengths up to 1.64 μ m. The uniaxial tensile strain effectively reduces the direct bandgap energy of the Ge NM, leading to a shift of the absorption edge toward a longer wavelength. Published by AIP Publishing. [<http://dx.doi.org/10.1063/1.4960460>]

Germanium (Ge) has been widely used in near infrared (NIR) photodetection on account of its large absorption coefficient at NIR wavelengths and compatibility with the modern Si CMOS technology.^{1–5} A flexible Ge photodetector is of great interest in recent years as it provides favorable characteristics such as light-weight, bendability, and robustness. The bendability property also enables the feasibility of non-flat imagers. A thin Ge layer was formed on flexible substrates via various transfer techniques in the past.^{6,7} In particular, single crystalline Ge nanomembranes (Ge NMs) released from Ge on the insulator (GeOI) wafer can offer a thickness range from tens to hundreds of nanometers.⁸ In addition, the doping type and doping concentration of the Ge NM can be controlled via the choice of its donor wafer and ion implantation beforehand. Metal-semiconductor-metal (MSM) photodiodes show great advantages such as low capacitance and easy integration.⁹ The MSM structure can be easily formed without using dopant diffusion such as ion implantation or spin-on dopant (SOD).¹⁰ However, large dark current is a critical drawback in Ge MSM photodiodes due to the small bandgap energy of Ge.^{11–13} Lightly doped Ge can be used in MSM photodiodes to overcome the large dark current because no ohmic contacts are required. Therefore, the combination of the lightly doped Ge NM and MSM structure could be an ideal solution for flexible Ge photodetectors. Although flexible Ge photodetectors with various device types (i.e., metal-insulator-semiconductor (MIS) and p-i-n (PIN)) have been reported, the bending effects on the photodetector characteristics have not been examined yet.^{6,7} Here, we report the fabrication and characterization of flexible Ge NM MSM photodiodes. GeOI wafer, a source material, was fabricated by wafer bonding and Smart-Cut[®] technology. The device was characterized on a bending fixture to examine strain-induced effects. The applied strain was quantified by Raman spectroscopy and NIR light with multiple wavelengths (i.e., 1.5, 1.55, 1.6, and 1.64 μ m) was focused on the device to measure the photo responsivity. We

investigated the correlation between the amount of strain and dark current and photo responsivity of the photodiode.

Four inch GeOI wafers were fabricated using a direct wafer bonding technique followed by the Smart-Cut[®] process.¹⁴ The fabrication began with unintentionally doped Ge wafer ($\rho > 40 \Omega \text{cm}$) which corresponds to a doping concentration of less than $3.7 \times 10^{13} \text{cm}^{-3}$. The detailed procedure of GeOI wafer fabrication can be found elsewhere.¹⁴ In short, hydrogen (H) ions (dose: $1 \times 10^{17} \text{cm}^{-2}$ and energy: 100 keV) were ion implanted on a Ge wafer capped with a 100 nm thick plasma enhanced chemical vapor deposition (PECVD) SiO₂, followed by the direct bonding with a Si wafer coated with a 200 nm thick thermal oxide. An 700 nm thick Ge layer was exfoliated from the Ge wafer and transferred onto the oxidized Si wafer using a two-step annealing process (200 °C for 3 h and 250 °C for 1 h). The rough Ge surface which was damaged during the implantation process was then chemically and mechanically polished and achieved a 400 nm Ge layer thickness with a 0.656 nm root mean square (RMS) surface roughness. Fig. 1(a) shows an optical image of the finished GeOI wafer.

Fig. 1(b) shows a schematic process flow of flexible Ge NM MSM photodiodes. The process began with the GeOI wafer (Fig. 1(b) i)) followed by the release and transfer of the Ge layer. A top Ge layer was patterned to an array of Ge islands (size: $40 \times 80 \mu\text{m}^2$) using reactive ion etching (RIE). A SiO₂ buried oxide layer was selectively etched by hydrofluoric acid (HF, 49%) and the Ge layer, now called Ge NM, was released and (Fig. 1(b) ii)) flip-transferred onto the adhesive layer (SU8-2002) coated polyethylene terephthalate (PET) substrate (Fig. 1(b) iii)). Interdigitated metal electrodes (Ti/Au = 50/450 nm) with a 2 μ m width and a 6 μ m distance between the electrodes were e-beam evaporated on the transferred Ge NMs and lifted off (Fig. 1(b) iv)). Figs. 1(c) and 1(d) show an optical image of flexible Ge NM MSM photodiodes on a bent PET substrate and a microscopic image of the array of the photodiodes, respectively.

The sample was mounted on convex fixtures with radius ranging from 77.5 to 21 mm. The strain created by fixtures was calculated by Horiba LabRAM ARAMIS Raman

^{a)}Current address: Department of Electrical and Computer Engineering, University of Illinois at Urbana-Champaign, Urbana, Illinois 61801, USA.

^{b)}Author to whom correspondence should be addressed. Electronic mail: mazq@engr.wisc.edu

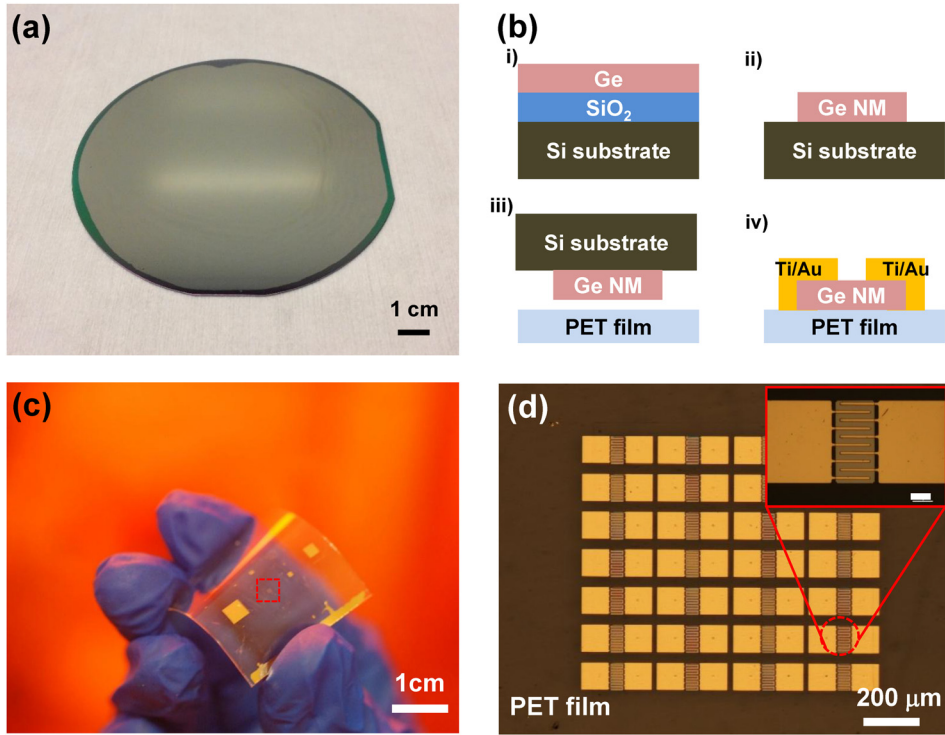


FIG. 1. (a) An optical image of the fabricated 4-in. GeOI wafer. (b) A schematic process flow for the Ge nanomembrane (Ge NM)-based metal-semiconductor-metal (MSM) photodiode on the flexible substrate: (i) Process begins with the fabrication of Ge on the insulator (GeOI) wafer with a 400 nm thick top Ge template layer and a 200 nm thick buried oxide layer. (ii) Ge NM released from the GeOI wafer using 49% hydrofluoric acid (HF). (iii) Ge NM transferred on the polyethylene terephthalate (PET) film coated with an adhesive layer (SU8-2002). (iv) Metal electrodes (Ti/Au = 50/450 nm) deposited by e-beam evaporation and lift-off. (c) An optical image of the array of Ge NM MSM photodiodes on a bent PET substrate. (d) A microscopic image of the flexible Ge NM MSM photodiodes on the PET substrate. The inset shows the image of an individual device. The scale bar in the inset is 20 μm .

spectroscopy. A 532 nm green laser was used to focus the surface of the Ge NM with a 100 \times objective lens. Fig. 2(a) shows the correlation between radii of the fixtures and induced tensile strain. The inset of Fig. 2(a) shows Raman spectra measured from the Ge NMs under the flat condition and bent PET substrate (Radius = 21 mm), respectively. The Raman scattering peak by the Ge-Ge vibration modes for the Ge NM appeared at 300.29 cm^{-1} without strain. The Ge Raman peaks measured under bending conditions were shifted to a smaller wavenumber, indicating that tensile strain was induced by the bending fixtures.

The uniaxial tensile strain in (001) Ge can be extracted based on the Raman shift using the following equation:¹⁵

$$\varepsilon(\%) = -0.495 \times \Delta\omega(\text{cm}^{-1}), \quad (1)$$

where ε is the uniaxial strain along the $\langle 110 \rangle$ direction and $\Delta\omega$ is the Raman peak shift. The Raman peak shifts of the Ge NMs bent along the $\langle 110 \rangle$ direction on the fixtures with radii of 77.5, 38.5, and 21 mm were measured to be 0.22,

0.46, and 0.84 cm^{-1} , respectively. Using Eq. (1), the uniaxial tensile strains of bent Ge NMs were calculated to be 0.11, 0.23, and 0.42%, respectively. Strain values extracted from Raman spectroscopy were confirmed with strain values associated with bending fixtures using the following equation:¹⁶

$$\varepsilon(\%) = \frac{1}{2R(\text{mm})/T(\mu\text{m}) + 1}, \quad (2)$$

where R is the radius of the fixture and T is the thickness of the bent object (μm). T includes the thicknesses of the PET film (175 μm), the adhesive layer (1 μm), and the Ge NM (0.4 μm). The uniaxial tensile strains corresponding to radii of 77.5, 38.5, and 21 mm were calculated to be 0.11, 0.23, and 0.42%, which agreed well with values from Raman results.

Fig. 2(b) shows the band diagram of the MSM photodiode under applied forward bias, which exceeds the flat-band voltage. When photons with larger energy than the bandgap of Ge (i.e., 0.66 eV) are absorbed, electron-hole pairs are generated and swept separately by the built-in electric field (See Fig. 2(b) i)). Since the absorption coefficient of Ge is greater under tensile strain,¹⁷ more electron-hole pairs are generated by the same condition, leading to increased photo currents (See Fig. 2(b) ii)). Also, a reduced Schottky barrier height (SBH) between the strained Ge NM and a metal contact is attributed to the split valence band, compared to the unstrained Ge. Change of SBH under mechanical strain can be calculated by the following equation:¹⁸

$$\Delta\phi_{bn}(\varepsilon) = \Delta\phi_m(\varepsilon) - \Delta\chi\varepsilon, \quad (3)$$

where ϕ_{bn} is the barrier height, ϕ_m is the metal work function, and χ is the electron affinity of the semiconductor. Since the change of the work function (ϕ_m) under the strain applied to devices is almost negligible, the change of the

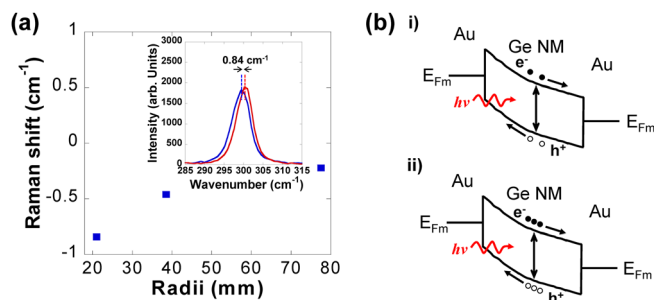


FIG. 2. (a) Raman shift corresponding to the radius of the bending fixture. The inset shows the Raman peak shift of 0.84 cm^{-1} measured from the Ge NMs under flat condition (red) and the fixture with a radius of 21 mm (blue). (b) The band diagram of the Ge NM based MSM photodiode: (i) without strain and (ii) under the tensile strain.

conduction band edge of the semiconductor is mainly attributed to the change of the SBH.¹⁸ According to Ref. 18, less than 0.01 eV of SBH reduction is expected under uniaxial tensile strain of 0.42%. The reduction in SBH represents less than 1% of SBH between Ti/Au and n-type Ge. Since SBH is significantly lowered by the forward bias, the effect of SBH reduction by tensile strain on photocurrent is almost negligible. Therefore, the percentage of the increased photocurrent caused by the change of SBH is nearly 0%. The increased photocurrent is mostly due to the enhanced absorption coefficient by tensile strain.

Current-voltage characteristics of Ge NM based MSM photodiodes were measured by a HP4155B semiconductor parameter analyzer under dark and illuminated conditions. An infrared light source with various wavelengths (i.e., 1.5, 1.55, 1.6, and 1.64 μm) from a tunable external cavity laser (TUNICS-Plus) was used to focus the devices via a lensed fiber. The output powers from the lensed fiber at different wavelengths were measured by a laser power meter (Edmund Coherent® FieldMate). The Ge NM photodiodes were initially characterized under the flat condition (i.e., without strain). Fig. 3(a) shows dark and photocurrent of the Ge NM photodiode at a bias range from 0 to 3 V. Fig. 3(b) shows the responsivity as a function of wavelength at 2 and 3 V voltage bias conditions. The responsivity values were measured to be 0.17 and 0.20 A/W under a wavelength of 1.5 μm at 2 and 3 V, respectively, which continuously decreased with increasing wavelength. This trend is ascribed to the sharp reduction of the absorption coefficient of Ge at 1.5 μm . Namely, the absorption coefficient of Ge is $5 \times 10^3 \text{ cm}^{-1}$ at 1.5 μm , and decreases to 60 cm^{-1} at 1.6 μm .¹⁹ Fig. 3(c) shows the responsivity as a function of optical power at 1.55 μm and $V = 2 \text{ V}$ and 3 V. As expected, the responsivity slightly decreased from 0.020 to 0.015 A/W at 3 V as the optical power is increased from 55 to 220 μW . However, the photocurrent at 1.55 μm linearly increased under the increasing optical powers (i.e., 55,

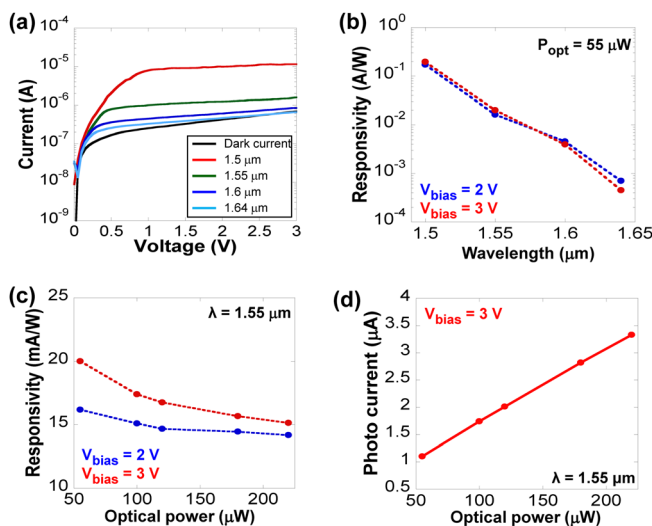


FIG. 3. (a) The measured dark and photo current at various wavelengths 1.5, 1.55, 1.6, and 1.64 μm . (b) Typical responsivity spectra of the photodiode as a function of wavelength without strain at 2 and 3 V. (c) Typical responsivity spectrum of the photodiode as a function of optical power at 1.55 μm without strain at 2 and 3 V. (d) The measured photo currents (wavelength: 1.55 μm) at 3 V with different optical powers of 55, 100, 120, 180, and 220 μW .

100, 120, 180, and 220 μW , respectively) as shown in Fig. 3(d). The result indicates that photo-generated carriers are responsible for the generated photocurrent under illumination.

To further investigate the correlation between the optical property and the strain, the performance changes of Ge NM photodiodes by the uniaxial tensile strain were evaluated. Fig. 4(a) shows the measured dark current density under various degrees of strain. The dark current density was measured to be 21.5 mA/cm^2 at 3 V without strain. It should be noted that the dark current density is lower than those of reported Ge MSM photodiodes which typically are on the order of 100 mA/cm^2 .²⁰ This low dark current density demonstrates the high quality of the transferred Ge NM. The dark current density constantly decreased to 14.8, 8.5, and 4.8 mA/cm^2 under the strain of 0.11, 0.23, and 0.42%, respectively. The suppression of the dark current was attributed to the splitting of the valence bands of Ge NM into light-hole (LH)/heavy-hole (HH) under the uniaxial tensile strain.²¹ Because the top of the valence band of Ge NM is composed of the LH band, intrinsic carrier density is decreased by the reduction of the density of states for holes, leading to the suppressed dark current.²² Although other groups claimed the opposite effect of tensile strain on dark current,^{23,24} their increased dark current is mainly attributed to dislocations in Ge layer introduced by growth of Ge on Si.

Fig. 4(b) shows the responsivity as a function of strain at wavelengths 1.5, 1.55, 1.6, and 1.64 μm . The responsivity was measured to be 0.2 A/W without strain, while it increased to 0.29, 0.3, and 0.45 A/W under 0.11, 0.23, and 0.42% strain, respectively, at 1.5 μm . In addition, the responsivity values were also enhanced at longer wavelengths as the strain is increased. Since the direct bandgap energy at the Γ valley decreases faster than the indirect bandgap energy at L valley under tensile strain, a relative enhancement in the optical property of Ge NM is expected. In order to examine the strain effect in Ge, the bandgap shrinkage was calculated using deformation potentials of Ge.²⁵ Theoretical calculation reveals that the energy difference between the Γ and L valleys is reduced from 133 meV (i.e., unstrained Ge) to 122 meV under 0.42% uniaxial tensile strain. The result suggests that an absorption edge of Ge expands toward lower energy (i.e., longer wavelength), allowing the detection range of the photodetector to cover a wavelength longer than 1.5 μm . Overall, tensile strained Ge NM based MSM photodiodes exhibit the enhancements in performance of not only low dark current but also high responsivity.

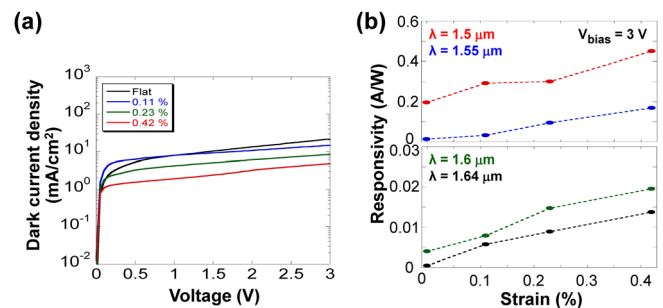


FIG. 4. (a) Dark current density versus voltage bias measured under uniaxial tensile strain. (b) Typical responsivity spectra as a function of the different strains at various wavelengths.

In summary, we have demonstrated flexible Ge NM based MSM photodiodes operating at a NIR range on the PET substrate. The optical and electrical characteristics of the uni-axial tensile strained photodiodes were investigated. The dark current density of the photodiode was reduced from 21.5 to 4.8 mA/cm² at 3 V, and the responsivity was increased from 0.2 to 0.45 A/W at 1.5 μ m by applying 0.42% strain. In addition, the enhancement in the responsivity was also observed at longer wavelengths up to 1.64 μ m. Improved performance such as dark current reduction and responsivity increase is ascribed to the bandgap shrinkage induced by tensile strain. The study indicates that mechanical strain can be used to enhance the performance of Ge photodetectors and, furthermore, Ge NM is suitable for making flexible NIR detectors with enhanced performance over rigid Ge wafer.

The work was supported by AFOSR under a PECASE Grant No. #FA9550-09-1-0482. The program manager is Dr. Gernot Pomrenke.

- ¹J. Michel, J. Liu, and L. C. Kimerling, *Nat. Photonics* **4**, 527–534 (2010).
- ²Y. Kang, H.-D. Liu, M. Morse, M. J. Paniccia, M. Zadka, S. Litski, G. Sarid, A. Pauchard, Y.-H. Kuo, H.-W. Chen, W. S. Zaoui, J. E. Bowers, A. Beling, D. C. McIntosh, X. Zheng, and J. C. Campbell, *Nat. Photonics* **3**, 59–63 (2009).
- ³D. Feng, S. Liao, P. Dong, N.-N. Feng, H. Liang, D. Zheng, C.-C. Kung, J. Fong, R. Shafiiha, J. Cunningham, A. V. Krishnamoorthy, and M. Asghari, *Appl. Phys. Lett.* **95**, 261105 (2009).
- ⁴L. Cao, J.-S. Park, P. Fan, B. Clemens, and M. L. Brongersma, *Nano Lett.* **10**(4), 1229–1233 (2010).
- ⁵M. Cho, J.-H. Seo, M. Kim, J. Lee, D. Liu, W. Zhou, Z. Yu, and Z. Ma, *J. Vac. Sci. Technol. B* **34**, 040604 (2016).
- ⁶W. S. Ho, Y.-H. Dai, Y. Deng, C.-H. Lin, Y.-Y. Chen, C.-H. Lee, and C. W. Liu, *Appl. Phys. Lett.* **94**, 261107 (2009).
- ⁷H.-Y. Yuan, J. Shin, G. Qin, L. Sun, P. Bhattacharya, M. G. Lagally, G. K. Celler, and Z. Ma, *Appl. Phys. Lett.* **94**, 013102 (2009).
- ⁸J. R. Sanchez-Perez, C. Boztug, F. Chen, F. F. Sudradjat, D. M. Paskiewicz, R. B. Jacobson, M. G. Lagally, and R. Paiella, *Proc. Natl. Acad. Sci. U.S.A.* **108**(47), 18893–18898 (2011).
- ⁹B. L. Sharma, *Metal-Semiconductor Schottky Barrier Junctions and Their Applications* (Plenum Press, NY, 1984).
- ¹⁰L. Colace, G. Masini, F. Galluzzi, G. Assanto, G. Capellini, L. D. Gaspare, E. Palange, and F. Evangelisti, *Appl. Phys. Lett.* **72**, 3175 (1998).
- ¹¹J. Oh, S. K. Banerjee, and J. C. Campbell, *IEEE Photonics Technol. Lett.* **16**(2), 581–583 (2004).
- ¹²K.-W. Ang, S.-Y. Zhu, J. Wang, K.-T. Chua, M.-B. Yu, G.-Q. Lo, and D.-L. Kwong, *IEEE Electron Device Lett.* **29**(7), 704–707 (2008).
- ¹³J. Kang, R. Zhang, M. Takenaka, and S. Takagi, *Opt. Express* **23**(13), 16967–16976 (2015).
- ¹⁴M. Kim, S.-C. Liu, T. Kim, J. Lee, J.-H. Seo, W. Zhou, and Z. Ma, *Opt. Express* **24**(15), 16894–16903 (2016).
- ¹⁵C.-Y. Peng, C.-F. Huang, Y.-C. Fu, Y.-H. Yang, C.-Y. Lai, S.-T. Chang, and C. W. Liu, *J. Appl. Phys.* **105**, 083537 (2009).
- ¹⁶G. Qin, L. Yang, J.-H. Seo, H.-C. Yuan, G. K. Celler, J. Ma, and Z. Ma, *Appl. Phys. Lett.* **99**, 243104 (2011).
- ¹⁷D. D. Cannon, J. Liu, Y. Ishikawa, K. Wada, D. T. Danielson, S. Jongthammanurak, J. Michel, and L. C. Kimerling, *Appl. Phys. Lett.* **84**, 906 (2004).
- ¹⁸M. H. Liao, P.-S. Kuo, S.-R. Jan, S. T. Chang, and C. W. Liu, *Appl. Phys. Lett.* **88**, 143509 (2006).
- ¹⁹E. D. Palik, *Handbook of Optical Constants of Solids* (Academic Press, NY, 1985).
- ²⁰H. Zang, S. J. Lee, W. Y. Loh, J. Wang, M. B. Yu, G. Q. Lo, D. L. Kwong, and B. J. Cho, *Appl. Phys. Lett.* **92**, 051110 (2008).
- ²¹J. R. Jain, A. Hryciw, T. M. Baer, D. A. B. Miller, M. L. Brongersma, and R. T. Howe, *Nat. Photonics* **6**, 398–405 (2012).
- ²²Y. Ishikawa, K. Wada, D. D. Cannon, J. Liu, H.-C. Luan, and L. C. Kimerling, *Appl. Phys. Lett.* **82**, 2044 (2003).
- ²³A. Okay, A. Nayfeh, K. Saraswat, N. Ozguven, A. Marshall, P. McIntyre, and T. Yonehara, in *IEEE LEOS* (2006), pp. 460–461.
- ²⁴J.-H. Yang, Y. Wei, X.-Y. Cai, and J.-Z. Ran, *Microelectron. Int.* **27**(2), 113–116 (2010).
- ²⁵C. G. Van der Walle, *Phys. Rev. B* **39**(3), 1871–1883 (1989).